

The picture of our universe: A view from modern cosmology

David D. Reid, Daniel W. Kittell, Eric E. Arsznov, and Gregory B. Thompson

Department of Physics and Astronomy, Eastern Michigan University, Ypsilanti,

MI 48197

In this paper we give a pedagogical review of the recent observational results in cosmology from the study of type Ia supernovae and anisotropies in the cosmic microwave background. By providing consistent constraints on the cosmological parameters, these results paint a concrete picture of our present-day universe. We present this new picture and show how it can be used to answer some of the basic questions that cosmologists have been asking for several decades. This paper is most appropriate for students of general relativity and/or relativistic cosmology.

I. INTRODUCTION

Since the time that Einstein pioneered relativistic cosmology, the field of cosmology has been dominated by theoretical considerations that have ranged from straightforward applications of well-understood physics to some of the most fanciful ideas in all of science. However, in the last several years observational cosmology has taken the forefront. In particular, the results of recent observations on high-redshift supernovae and anisotropies in the radiation from the cosmic microwave background (CMB) have pinned down the major cosmological parameters to sufficient accuracy that a precise picture of our universe has now emerged. In this paper, we present this picture as currently suggested by the beautiful marriage of theory and experiment that now lies at the heart of modern cosmology.

We begin our discussion, in sections II and III, with a review of the standard theory of the present-day universe that persisted, virtually unaltered, from the time of Einstein until the mid 1990s. This review will lay most of the theoretical groundwork needed for sections

IV and V on the two experimental efforts that has had such a major impact over the last few years. Once the new results have been explained, we present, in section VI, the picture of our universe that has emerged from the recent results. We then conclude this paper with some brief comments on the implications of these results for our understanding of not just the present-day universe, but of its past and future. To help make this discussion more accessible, we use SI units with time measured in seconds instead of meters and with all factors of G and c explicitly shown unless otherwise noted.

II. REVIEW OF THE STANDARD PRESENTATION OF COSMOLOGY

The basic tenet that governs cosmology is known as the *cosmological principle*. This principle states that, on large scales, the present universe is homogeneous and isotropic. Homogeneity means that the properties of the universe are the same everywhere in the universe; and isotropy means that from every point, the properties of the universe are the same in every direction. It can be shown that the cosmological principle alone requires that the metric tensor of the universe must take the form of the Robertson-Walker metric [1]. In co-moving, spherical coordinates, this metric tensor leads to the well known line element

$$ds^2 = c^2 dt^2 - a^2(t) \left[\frac{dr^2}{1 - kr^2} + r^2 d\theta^2 + r^2 \sin^2 \theta d\phi^2 \right], \quad (1)$$

where the dimensionless function $a(t)$ is called the cosmic scale factor. This line element describes an expanding (or contracting) universe that, at the present (or any) instant in time t_0 , is a three-dimensional hypersphere of constant scalar curvature $K(t_0) = k/a^2(t_0)$. The parameter k represents the sign of this constant which can either be positive ($k = +1 \text{ m}^{-2}$), negative ($k = -1 \text{ m}^{-2}$), or zero ($k = 0$).

The dynamics of the universe is governed by the Einstein field equations

$$R_{\mu\nu} - \frac{1}{2}g_{\mu\nu}R = \frac{8\pi G}{c^4}T_{\mu\nu}, \quad (2)$$

where $R_{\mu\nu}$ is the Ricci tensor, R is the scalar curvature, and $T_{\mu\nu}$ is the stress-energy tensor.

On large scales, the stress-energy tensor of the universe is taken to be that of a perfect fluid (since homogeneity and isotropy imply that there is no bulk energy transport)

$$T_{\mu\nu} = (p + \rho)u_\mu u_\nu / c^2 - pg_{\mu\nu}, \quad (3)$$

where u_μ is the four-velocity of the fluid, ρ is its energy density, and p is the fluid pressure. In Eqs. (2) and (3), $g_{\mu\nu}$ is relative to the Cartesian coordinates ($x^0 = ct, x^1 = x, x^2 = y, x^3 = z$).

Under the restrictions imposed by the cosmological principle, the field equations (2) reduce to the Friedmann equations for the cosmic scale factor

$$\frac{\ddot{a}}{a} = -\frac{4\pi G}{3c^2}(\rho + 3p) \quad (4)$$

$$\left(\frac{\dot{a}}{a}\right)^2 = \frac{8\pi G}{3c^2}\rho - \frac{kc^2}{a^2}, \quad (5)$$

where the dot notation represents a derivative with respect to time, as is customary. Observationally, it is known that the universe is expanding. The expansion of the universe follows the Hubble law

$$v_r = \frac{\dot{a}}{a}d = Hd, \quad (6)$$

where v_r is the speed of recession between two points, d is the proper distance between these points, and H ($\equiv \dot{a}/a$) is called the *Hubble parameter*. One of the key features of the Hubble law is that, at any given instant, the speed of recession is directly proportional to the distance. Therefore, by analyzing the Doppler shift in the light from a distant source we can infer its distance provided that we know the present value of the Hubble parameter H_0 , called the *Hubble constant* [2].

One of the principal questions that the field of cosmology hopes to answer concerns the ultimate fate of the universe. Will the universe expand forever, or will the expansion halt and be followed by a contraction? This question of the long-term fate of the expansion is closely connected to the sign of k in the Friedmann equation (5). General relativity teaches us that the curvature of spacetime is determined by the density of matter and energy. Therefore,

the two terms on the right-hand-side of Eq. (5) are not independent. The value of the energy density will determine the curvature of spacetime and, consequently, the ultimate fate of the expansion. Recognizing that the left-hand-side of Eq. (5) is H^2 , we can rewrite this expression as

$$1 = \frac{8\pi G\rho}{3c^2 H^2} - \frac{kc^2}{H^2 a^2}, \quad (7)$$

and make the following definition:

$$\Omega \equiv \frac{8\pi G\rho}{3c^2 H^2}, \quad (8)$$

called the *density parameter*.

Since the sum of the density and curvature terms in Eq. (7) equals unity, the case for which $\Omega < 1$ corresponds to a negative curvature term requiring $k = -1 \text{ m}^{-2}$. The solution for negative curvature is such that the universe expands forever with excess velocity $\dot{a}_{t=\infty} > 0$. This latter case is referred to as an *open* universe. The case for which $\Omega > 1$ corresponds to a positive curvature term requiring $k = +1 \text{ m}^{-2}$. The solution for positive curvature (a *closed* universe) is such that the expansion eventually halts and becomes a universal contraction leading to what is known as the *big crunch*. Finally, the case for which $\Omega = 1$ corresponds to zero curvature (a *flat* universe) requiring $k = 0$. The solution for a flat universe is the critical case that lies on the boundary between an open and closed universe. In this case, the universe expands forever, but the rate of expansion approaches zero asymptotically, $\dot{a}_{t=\infty} = 0$. The value of the energy density for which $\Omega = 1$ is called the *critical density* ρ_c , given by

$$\rho_c = \frac{3c^2 H^2}{8\pi G}. \quad (9)$$

The density parameter, then, is the ratio of the energy density of the universe to the critical density $\Omega = \rho/\rho_c$.

There is one final parameter that is used to characterize the universal expansion. Notice that Eq. (4) expresses the basic result that in a matter-dominated universe (in which $\rho + 3p >$

0) the expansion should be decelerating, $\ddot{a} < 0$, as a result of the collective gravitational attraction of the matter and energy in the universe. This behavior is characterized by the *deceleration parameter*

$$q \equiv -\frac{\ddot{a} a}{\dot{a}^2}. \quad (10)$$

The matter in the present universe is very sparse, so that it is effectively noninteracting (i.e., dust). Therefore, it is generally assumed that the fluid pressure, p , is negligible compared to the energy density. Under these conditions, Eq. (4) shows that the deceleration parameter has a straightforward relationship to the density parameter

$$q = \Omega/2. \quad (11)$$

Collectively, the Hubble constant H_0 and the present values of the density parameter Ω_0 and the deceleration parameter q_0 are known as the *cosmological parameters*. These parameters are chosen, in part, because they are potentially measurable. The range of values that correspond to the different fates of the universe, within this traditional framework, are summarized in Table 1.

TABLE 1. The ranges of the main cosmological parameters for the three models of the universe in the standard presentation of cosmology

Model	Parameters		
	$50 < H_0 < 100 \text{ km}\cdot\text{s}^{-1}\cdot\text{Mpc}^{-1}$		
Open	$\Omega < 1$	$\rho_m < \rho_c$	$q_0 < 1/2$
Closed	$\Omega > 1$	$\rho_m > \rho_c$	$q_0 > 1/2$
Flat	$\Omega = 1$	$\rho_m = \rho_c$	$q_0 = 1/2$

The understanding of cosmology, as outlined above, left several questions unanswered, including the fate of the universal expansion. It was entirely possible to formulate reasonable arguments for whether or not the universe is open, closed, or flat that covered all three

possibilities. The observational data has always suggested that the density of visible matter is insufficient to close the universe and researchers choosing to side with the data could easily take the position that the universe is open. However, it has been known for several decades that a substantial amount of the matter in the universe, perhaps even most of it, is not visible. The existence of large amounts of *dark matter* can be inferred from its gravitational effects both on and within galaxies [3]. Therefore, the prospects of dark matter (and neutrino mass) rendered any conclusion based solely on the amount of visible matter premature. Einstein's view was that the universe is closed, apparently for reasons having to do with Mach's principle [4], and many researchers preferred this view as well for reasons that were sometimes more philosophical than scientific. Then, there were also hints that the universe may be flat; consequentially, many researchers believed that this was most likely true.

Belief that the universe is flat was partly justified by what is known in cosmology as the *flatness problem* having to do with the apparent need of the universe to have been exceedingly close to the critical density shortly after the big bang. The fate of the universe and the flatness problem are just two of several puzzles that emerge from this standard model of the universe. Another important puzzle has to do with the existence, or nonexistence, of the *cosmological constant*, Λ . It turns out that Λ plays a very important role in our story, and *its* story must be told before we can explain how cosmologists have pinned down some of the basic properties of the universe.

III. THE COSMOLOGICAL CONSTANT

In 1915 Albert Einstein introduced his theory of General Relativity. Like Newton before him, Einstein's desire was to apply his theory to cosmology. Einstein embraced the prevailing view at that time that the universe is static. Therefore, he attempted to find solutions of the form $\dot{a}=0$. It soon became apparent that even with Einstein's theory of gravity, as with Newton's, the gravitational attraction of the matter in the universe causes a static universe

to be unstable. Furthermore, as can be seen from Eq. (4), the subsequent requirement of $\ddot{a}=0$ implies a negative pressure such that $p = -\rho/3$. For ordinary stellar matter and gas, this relationship is not physically reasonable.

To remedy such problems, Einstein modified his original field equations from Eq. (2) to the more general form

$$R_{\mu\nu} - \frac{1}{2}g_{\mu\nu}R - \Lambda g_{\mu\nu} = \frac{8\pi G}{c^4}T_{\mu\nu}, \quad (12)$$

where Λ is the cosmological constant mentioned in the previous section. Equation (12) is the most general form of the field equations that remains consistent with the physical requirements of a relativistic theory of gravity. The cosmological constant term, for $\Lambda > 0$, can be viewed as a repulsive form of gravity that is independent of the curvature of spacetime. The modern approach is to treat Λ as a form of energy present even in empty space - vacuum energy [5]. This interpretation implies modifying Eq. (12) to

$$R_{\mu\nu} - \frac{1}{2}g_{\mu\nu}R = \frac{8\pi G}{c^4} \left(T_{\mu\nu} + \frac{\Lambda c^4}{8\pi G} g_{\mu\nu} \right). \quad (13)$$

In the perfect fluid approximation, this leads to an effective fluid pressure and energy density given by

$$p = p_m - \frac{\Lambda c^4}{8\pi G} \quad (14)$$

$$\rho = \rho_m + \frac{\Lambda c^4}{8\pi G}, \quad (15)$$

where p_m and ρ_m are the pressure and energy density of the *matter* content of the universe. As Eq. (14) shows, the cosmological constant contributes a negative term to the pressure in the universe. This affect of the cosmological constant allowed Einstein to find a static, albeit unstable, solution for the dynamics of the universe.

Once it became known that the universe is expanding, Einstein discarded the cosmological constant term having no other physical reason to include it. However, the possible existence of a non-zero cosmological constant has been a subject of debate ever since. With

the cosmological constant in the picture, the equations for the dynamics of the universe, Eqs. (4) and (5), generalize to

$$\frac{\ddot{a}}{a} = -\frac{4\pi G}{3c^2}(\rho_m + 3p_m) + \frac{\Lambda c^2}{3} \quad (16)$$

$$\left(\frac{\dot{a}}{a}\right)^2 = H^2 = \frac{8\pi G}{3c^2}\rho_m - \frac{kc^2}{a^2} + \frac{\Lambda c^2}{3}. \quad (17)$$

Besides Einstein's static model of the universe, another interesting, and important, solution to Eqs. (16) and (17), known as the *de Sitter solution*, applies to the case of a spatially flat, empty universe ($\rho_m = 0$, $p_m = 0$, $k = 0$). In this case, Λ supplies the only contribution to the energy density

$$\rho = -p = \frac{\Lambda c^4}{8\pi G}. \quad (18)$$

Equation (16) shows that under these conditions the universe would be accelerating $\ddot{a} > 0$, and Eq. (17) shows that the Hubble parameter would be given by

$$H = \left(\frac{\Lambda c^2}{3}\right)^{1/2}. \quad (19)$$

The de Sitter solution for the cosmic scale factor shows that the effect of the cosmological constant is to cause the accelerating universe to expand exponentially with time according to

$$a(t) = a_0 e^{Ht}. \quad (20)$$

Obviously, the universe is not completely empty, but the de Sitter solution remains important because it is possible for a cosmological constant term to be sufficiently large as to dominate the dynamics of the universe. The dominant components of the universe are determined by the relative values of the corresponding density parameters. Dividing Eq. (17) by H^2 produces the analog of Eq. (7)

$$1 = \frac{8\pi G\rho_m}{3H^2c^2} + \frac{kc^2}{a^2H^2} + \frac{\Lambda c^2}{3H^2}, \quad (21)$$

where the sign of k has been separated out. The first term on the right-hand-side is called the matter term and, in analogy with Eq. (8), also gives the matter density parameter Ω_m . The second term is the curvature term and is characterized by the curvature density parameter Ω_k . Finally, the last term is known as the vacuum-energy density parameter Ω_Λ . Thus, in a universe with a cosmological constant, the primary density parameters are

$$\Omega_m = \frac{8\pi G\rho_m}{3H^2c^2}, \quad \Omega_k = -\frac{kc^2}{a^2H^2}, \quad \Omega_\Lambda = \frac{\Lambda c^2}{3H^2}. \quad (22)$$

The present values of these parameters, together with the Hubble constant, would determine the dynamics of the universe in this model [6].

IV. DETERMINING COSMOLOGICAL PARAMETERS FROM TYPE IA SUPERNOVAE

A. Type Ia Supernovae

Throughout their lives, stars remain in stable (hydrostatic) equilibrium due to the balance between outward pressures (from the fluid and radiation) and the inward pressure due to the gravitational force. The enormously energetic nuclear fusion that occurs in stellar cores causes the outward pressure. The weight of the outer region of the star causes the inward pressure. A supernova occurs when the gravitational pressure overcomes the internal pressure, causing the star to collapse, and then violently explode. There is so much energy released (in the form of light) that we can see these events out to extremely large distances.

Supernovae are classified into two types according to their spectral features and light curves (plot of luminosity vs. time). Specifically, the spectra of type Ia supernovae are hydrogen-poor, and their light curves show a sharp rise with a steady, gradual decline. In addition to these spectroscopic features, the locations of these supernovae, and the absence of planetary nebulae, allow us to determine the genesis of these events. Based on these facts, it is believed that the progenitor of a type Ia supernova is a binary star system consisting

of a *white dwarf* with a *red giant* companion [7]. Other binary systems have been theorized to cause these supernovae, but are not consistent with spectroscopic observation [8].

Although the Sun is not part of a binary system, approximately half of all stellar systems are. Both members are gravitationally bound and therefore revolve around each other. While a binary star system is very common, the members of the progenitor to a type Ia supernova have special properties. White dwarf stars are different from stars like the Sun in that nuclear fusion does not take place within these objects. Electron degeneracy pressure, which is related to the well known Pauli exclusion principle, holds the white dwarf up against its own weight. For electron degeneracy pressure to become important, an object must be extremely dense. White dwarf stars have the mass of the Sun, but are the size of the Earth. Also, the physics of this exotic form of pressure produces a strange effect: heavier white dwarfs are actually smaller in size ($\text{mass} \times \text{volume} = \text{constant}$) [9]. Red giant stars, on the other hand, are the largest known stars and contain a relatively small amount of mass. As a result, gravity is relatively weak at the exterior region of red giant stars.

In such a binary system, the strong gravitational attraction of the white dwarf overcomes the weaker gravity of the red giant. At the outer edge of the red giant, the gravitational force from the white dwarf is stronger than that from the red giant. This causes mass from the outer envelope of the red giant to be accreted onto the white dwarf. As a result, the mass of the white dwarf increases, causing its size to decrease. This process continues until the mass of the white dwarf reaches the *Chandrasekhar limit* (1.44 solar masses) beyond which electron degeneracy pressure is no longer able to balance the increasing pressure due to the gravitational force. At the center of the white dwarf, the intense pressure and temperature ignites the fusion of Carbon nuclei. This sudden burst of energy produces an explosive deflagration (subsonic) wave that destroys the star. This violently exploding white dwarf is what we see as a type Ia supernova.

The use of type Ia supernovae for determining cosmological parameters rests on the ability of these supernovae to act as standard candles. Standard candles have been used to determine distances to celestial objects for many years. They are luminous objects whose

intrinsic (or absolute) brightness can be determined independent of their distance. The intrinsic brightness, together with the observed apparent brightness (which depends on the distance to the object), can be used to calculate distances. The distance calculated from measurements of the luminosity (power output) of an object is appropriately termed the *luminosity distance*

$$d = 10^{(m-M-25)/5}, \quad (23)$$

where m is the apparent brightness measured in magnitudes (apparent magnitude), M is the absolute magnitude, and d is the luminosity distance in units of megaparsecs. The quantity, $m - M$ is commonly known as the *distance modulus*. For the reader who is unfamiliar with the magnitude scale see chapter 3 of Ref. 9.

As explained above, all type Ia supernovae are caused by the same process, a white dwarf reaching 1.44 solar masses by accretion from a red giant. As a result of this consistency, we not only expect to see extremely consistent light curves from these events, but we also expect that these light curves will reach the same peak magnitude. If this latter point is true, type Ia supernovae can be used as standard candles and, therefore, distance indicators.

Methods for determining the absolute magnitude of a type Ia supernova can be divided into two categories depending on whether or not we know the distance to the event. If we know the distance to the host galaxy of the supernova, by means of a Cepheid variable for example, and we observe the apparent magnitude of the event m , then we can use the distance modulus to calculate the absolute magnitude directly

$$m - M = 5 \log(d) + 25. \quad (24)$$

If the distance is not known, the peak luminosity must be inferred from observational data. The techniques for making this inference often involve corrections for many processes that would otherwise adversely affect the results. These processes include interstellar extinction within the host galaxy, redshift of the light from the expansion of the universe, gravitational lensing, and an apparently natural scatter in the peak brightness; see Ref. 10 for a discussion of these corrections. Once the luminosity L of a supernova has been determined, this

luminosity, together with the luminosity L' , and absolute magnitude M' , of a well-known object (such as the Sun) will yield the absolute magnitude of the supernova

$$M = M' - 2.5 \log(L/L'). \quad (25)$$

Taking all of this into account, it has been determined that the peak absolute magnitude of type Ia supernovae is [11]

$$M_{Ia} = -19.5 \pm 0.2 \text{ mag.} \quad (26)$$

B. Measuring the Hubble Constant

As stated previously, the expansion of the universe follows the Hubble law given by Eq. (6). Observationally, we measure the recession velocity as a redshift, z , in the light from the supernova ($v_r = cz$). Since every type Ia supernovae has about the same absolute magnitude, Eq. (26), the apparent magnitude provides an indirect measure of its distance. Therefore, for nearby supernovae ($z \leq 0.3$) the Hubble Law is equivalent to a relationship between the redshift and the magnitude. Inserting (26) into (24), using (6), and applying to the current epoch, yields the *redshift-magnitude relation*

$$m = M_{Ia} + 5 \log(cz) - 5 \log(H_0) + 25. \quad (27)$$

Defining the $z = 0$ intercept as

$$\tilde{M} \equiv M_{Ia} - 5 \log(H_0) + 25, \quad (28)$$

we can write equation (27) as

$$m = \tilde{M} + 5 \log(cz). \quad (29)$$

As shown in Fig. 1, low-redshift data can be used to find \tilde{M} and Eq. (28) to solve for the Hubble constant. Studies on type Ia supernova [12] consistently suggest a value for the Hubble constant of about $63 \text{ km}\cdot\text{s}^{-1}\cdot\text{Mpc}^{-1}$.

The result for H_0 , found from low-redshift supernovae, tends to set the lower bound when compared with other methods for obtaining H_0 . For example, if the distances to enough galaxies can be accurately found, then the Hubble law can be used directly to obtain a value of H_0 . This has partly been the goal of the *Hubble Space Telescope Key Project* [13]. This project has shown that a careful consideration of the type Ia supernova results in combination with the other methods for obtaining H_0 produces what has become a widely accepted value for the Hubble constant

$$H_0 = 72 \pm 8 \text{ km} \cdot \text{s}^{-1} \cdot \text{Mpc}^{-1}. \quad (30)$$

The value given in Eq. (30) is the one that we shall adopt in this paper.

C. Measuring Ω_m , Ω_Λ , and q_0

In order to determine the other cosmological parameters from the supernova data we must consider supernova at large distances ($z \geq 0.3$). Just as large distance measurements on Earth show us the curvature (geometry) of Earth's surface, so do large distance measurements in cosmology show us the geometry of the universe. Since, as we have seen, the geometry of the universe depends on the values of the cosmological parameters, measurements of the luminosity distance for distant supernova can be used to extract these values.

To obtain the general expression for the luminosity distance, consider photons from a distant source moving radially toward us. Since we are considering photons, $ds^2 = 0$, and since they are moving radially, $d\theta^2 = d\phi^2 = 0$. The Robertson-Walker metric, Eq. (1), then reduces to $0 = c^2 dt^2 - a^2 dr^2 (1 - kr^2)^{-1}$, which implies

$$dt = \frac{adr}{c(1 - kr^2)^{1/2}}. \quad (31)$$

To get another expression for dt , we multiply Eq. (17) by $a^2(t)$ which produces an expression for $(da/dt)^2$. Furthermore, we note that since the universe is expanding, the matter density is a function of time. Given that lengths scale as $a(t)$, volumes scale as $a^3(t)$ and therefore,

$$\rho_m(t) \propto 1/a^3(t). \quad (32)$$

Using these facts, together with the definitions of the density parameters in Eq. (22), Eq. (17) becomes

$$\left(\frac{da}{dt}\right)^2 = H_0^2 \left[\Omega_{m,0} \frac{a_0}{a} + \Omega_{k,0} + \Omega_{\Lambda,0} \left(\frac{a}{a_0}\right)^2 \right]. \quad (33)$$

As previously mentioned, it is better to write things in terms of measurable quantities, and in this case we can directly relate the cosmic scale factor to the redshift z . The redshift is defined such that

$$1 + z = \frac{\lambda_0}{\lambda}, \quad (34)$$

where λ_0 is the current (received) value of the wavelength and λ is the wavelength at the time of emission. The redshift is a direct result of the cosmic expansion and it can be shown that [14] $\lambda \propto a(t)$; therefore,

$$\frac{a_0}{a} = 1 + z. \quad (35)$$

Using Eq. (35) and the fact that $\Omega_k = 1 - \Omega_m - \Omega_\Lambda$ from Eq. (21), Eq. (33) can be rewritten as

$$dt = H_0^{-1} (1+z)^{-1} \left[(1+z)^2 (1 + \Omega_{m,0} z) - z(z+2)\Omega_{\Lambda,0} \right]^{-1/2} dz. \quad (36)$$

Equating the expressions in Eqs. (31) and (36) and integrating, leads to an expression for the radial coordinate r of the star. The luminosity distance is then given by [15] $d = (1+z)a_0 r$. Therefore,

$$d = \frac{c(1+z)}{H_0 |\Omega_{k,0}|^{1/2}} \text{sinn} \left\{ |\Omega_{k,0}|^{1/2} \int_0^z \left[(1+z')^2 (1 + \Omega_{m,0} z') - z'(z'+2)\Omega_{\Lambda,0} \right]^{-1/2} dz' \right\}, \quad (37)$$

where $\text{sinn}(x)$ is $\sinh(x)$ for $k < 0$, $\sin(x)$ for $k > 0$, and if $k = 0$ neither sinn nor $|\Omega_{k,0}|$ appear in the expression. We see that the functional dependence of the luminosity distance is $d(z; \Omega_m, \Omega_\Lambda)$.

Inserting Eq. (37) into Eq. (24), and using the intercept from Eq. (28), we get a redshift-magnitude relation valid at high z

$$m - \tilde{M} = 5 \log[d(z; \Omega_m, \Omega_\Lambda)] \quad (38)$$

In practice, astronomers observe the apparent magnitude and redshift of a distant supernova. The density parameters are then determined by those values that produce the best fit to the observed data according to Eq. (38) for different cosmological models.

Under the continued assumption that the fluid pressure of the matter in the universe is negligible ($p_m \approx 0$), Eq. (16) implies that the deceleration parameter at the present time is given by

$$q_0 = \Omega_{m,0}/2 - \Omega_{\Lambda,0}. \quad (39)$$

Therefore, once the density parameters have been determined by the above procedure, the deceleration parameter can then be found.

Figure 2 illustrates how high-redshift data can be used to estimate the cosmological parameters and provide evidence in favor of a nonzero cosmological constant. In this figure, the abscissa is the difference between the distance moduli for the observed supernovae and what would be expected for a traditional cosmological model such as those represented in Table 1. The case shown is based on the data of Riess *et. al.* [16] using a traditional model with $\Omega_m = 0.2$ and $\Omega_\Lambda = 0$ represented by the central line $\Delta(m - M) = 0$. The figure shows that the data points lie predominantly above the zero line. This result means that the supernovae are further away (or equivalently, dimmer) than traditional, decelerating cosmological models allow. The conclusion then is that the universe must be accelerating. As suggested by Eq. (39), the most straightforward explanation of this conclusion is the presence of a nonzero, positive cosmological constant. The solid curve, above the zero line in Fig. 2, represents a best-fit curve to the data that corresponds to a universe with $\Omega_m = 0.24$ and $\Omega_\Lambda = 0.72$.

Typical values for the cosmological parameters as determined by detailed analysis of the type just discussed are the following [16]:

$$\begin{aligned}
\Omega_{m,0} &= 0.24_{-0.24}^{+0.56} \\
\Omega_{\Lambda,0} &= 0.72_{-0.48}^{+0.72} \\
q_0 &= -1.0 \pm 0.4.
\end{aligned}
\tag{40}$$

Note that the negative deceleration parameter is consistent with an accelerating universe. Furthermore, these values imply that the universe is effectively flat predicting a curvature parameter roughly centered around $\Omega_k \approx 0.04$.

V. DETERMINING COSMOLOGICAL PARAMETERS FROM ANISOTROPIES IN THE CMB

The theory of the anisotropies in the CMB is rich with details about the contents and structure of the early universe. Consequently, this theory can become quite complicated. However, because of this same richness, this branch of cosmology holds the potential to provide meaningful constraints on a very large number of quantities of cosmological interest. Our focus here is to provide the reader with a conceptual understanding of why and how CMB anisotropies can be used to determine cosmological parameters. We will place particular emphasis on the density parameters corresponding to the spatial curvature of the universe Ω_k , and the baryon density Ω_b . The reader seeking more detail should consult Ref. 17 and the references therein.

A. Anisotropies in the CMB

The “hot big bang” model is widely accepted as the standard model of the early universe. According to this idea, our universe started in a very hot, very dense state that suddenly began to expand, and the expansion is continuing today. All of space was contained in that dense point. It is not possible to observe the expansion from an outside vantagepoint and it is not correct to think of the big bang as happening at one point in space. The big bang happened everywhere at once.

During the first fraction of a second after the big bang, it is widely believed that the universe went through a brief phase of exponential expansion called *inflation* [18]. Baryonic matter formed in about the first second; and the nuclei of the light elements began to form (nucleosynthesis) when the universe was only several minutes old. Baryons are particles made up of three quarks; the most familiar baryons are the protons and neutrons in the nuclei of atoms. Since all of the matter that we normally encounter is made up of atoms, baryonic matter is considered to be the “ordinary” matter in the universe.

The very early universe was hot enough to keep matter ionized, so the universe was filled with nucleons and free electrons. The density of free electrons was so high that Thomson scattering effectively made the universe opaque to electromagnetic radiation. The universe remained a baryonic plasma until around 300,000 years after the big bang when the universe had expanded and cooled to approximately 3000 K. At this point, the universe was sufficiently cool that the free electrons could join with protons to form neutral hydrogen. This process is called *recombination*. With electrons being taken up by atoms, the density of free electrons became sufficiently low that the mean free path of the photons became much larger (on the order of the size of the universe); and light was free to propagate. The light that was freed during recombination has now cooled to a temperature of about $T_o = 2.73$ K. This light is what we observe today as the cosmic microwave background. We see the CMB as if it were coming from a spherical shell called the *surface of last scattering* (Fig. 3). This shell has a finite thickness because recombination occurred over a finite amount of time.

Today, over very large scales, the universe is homogeneous. However, as evidenced by our own existence, and the existence of galaxies and groups of galaxies, etc., inhomogeneities exist up to scales on the order of 100 Mpc. Theories of structure formation require that the seeds of the structure we observe today must have been inhomogeneities in the matter density of the early universe. These inhomogeneities would have left their imprint in the CMB which we would observe today as temperature anisotropies. So, in order to explain the universe in which we live, there should be bumps in the CMB; and these bumps should occur over angular scales that correspond to the scale of observed structure. In 1992, the

COBE satellite measured temperature fluctuations δT in the CMB, $\delta T/T \sim 10^{-5}$ on a 7° angular scale [19], where T is the ambient temperature of the CMB. The anisotropies detected by COBE are considered to be large-scale variations caused by nonuniformities generated at the creation of the universe. However, recent observations [20-22] have found small-scale anisotropies that correspond to the physical scale of today's observed structure. It is believed that these latter anisotropies are the result of quantum fluctuations in density that existed prior to inflation which were greatly amplified during inflation. These amplified fluctuations became the intrinsic density perturbations which are the seeds of structure formation.

The small-scale anisotropies in the CMB can be separated into two categories: primary and secondary. Primary anisotropies are due to effects that occur at the time of recombination and are “imprinted” in the CMB as the photons leave the surface of last scattering. Secondary anisotropies arise through scattering along the line of sight between the surface of last scattering and the observer. In this paper, we will only be concerned with the primary anisotropies. There are three main sources for primary anisotropies in the microwave background. These are the Sachs-Wolfe effect, intrinsic (adiabatic) perturbations, and a Doppler effect.

For the largest of these primary anisotropies the dominant mechanism is the Sachs-Wolfe effect. At the surface of last scattering, matter density fluctuations will lead to perturbations in the gravitational potential, $\delta\Phi$. These perturbations cause a gravitational redshift of the photons coming from the surface of last scattering as they “climb out” of the potential wells. This effect is described by, $\delta T/T = \delta\Phi/c^2$. These same perturbations in the gravitational potential also cause a time dilation at the surface of last scattering, so these photons appear to come from a younger, hotter universe. This effect is described by, $\delta T/T = -2(\delta\Phi)/3c^2$. Combining these two processes gives the Sachs-Wolfe effect [23],

$$\frac{\delta T}{T} = \frac{\delta\Phi}{3c^2}. \quad (41)$$

On intermediate scales, the main effect is due to adiabatic perturbations. Recombination

occurs later in regions of higher density, so photons emanating from overly dense regions experience a smaller redshift from the universal expansion and thus appear hotter. The observed temperature anisotropy resulting from this process is given by [23],

$$\left(\frac{\delta T}{T}\right)_{obs} = -\frac{\delta z}{1+z} = \frac{\delta\rho}{\rho}. \quad (42)$$

Finally, on smaller scales there is a Doppler effect that becomes important. This effect arises because the photons are last scattered in a moving plasma. The temperature anisotropy corresponding to this effect is described by [23],

$$\frac{\delta T}{T} = \frac{\delta\vec{v} \cdot \hat{r}}{c}, \quad (43)$$

where \hat{r} denotes the direction along the line of sight and \vec{v} is a characteristic velocity of the material in the scattering medium.

B. Acoustic Peaks and the Cosmological Parameters

The early universe was a plasma of photons and baryons and can be treated as a single fluid [24]. Baryons fell into the gravitational potential wells created by the density fluctuations and were compressed. This compression gave rise to a hotter plasma thus increasing the outward radiation pressure from the photons. Eventually, this radiation pressure halted the compression and caused the plasma to expand (rarefy) and cool producing less radiation pressure. With a decreased radiation pressure, the region reached the point where gravity again dominated and produced another compression phase. Thus, the struggle between gravity and radiation pressure set up longitudinal (acoustic) oscillations in the photon-baryon fluid. When matter and radiation decoupled at recombination the pattern of acoustic oscillations became frozen into the CMB. Today, we detect the evidence of the sound waves (regions of higher and lower density) via the primary CMB anisotropies.

It is well known that any sound wave, no matter how complicated, can be decomposed into a superposition of wave modes of different wavenumbers k , each k being inversely

proportional to the physical size of the corresponding wave (its wavelength), $k \propto 1/\lambda$. Observationally, what is seen is a projection of the sound waves onto the sky. So, the wavelength of a particular mode λ is observed to subtend a particular angle θ on the sky. Therefore, to facilitate comparison between theory and observation, instead of a Fourier decomposition of the acoustic oscillations in terms of sines and cosines, we use an angular decomposition (multipole expansion) in terms of Legendre polynomials $P_\ell(\cos\theta)$. The order of the polynomial ℓ (related to the multipole moments) plays a similar role for the angular decomposition as the wavenumber k does for the Fourier decomposition. For $\ell \geq 2$ the Legendre polynomials on the interval $[-1,1]$ are oscillating functions containing a greater number of oscillations as ℓ increases. Therefore, the value of ℓ is inversely proportional to the characteristic angular size of the wave mode it describes

$$\ell \propto 1/\theta. \tag{44}$$

Experimentally, temperature fluctuations can be analyzed in pairs, in directions \hat{n} and \hat{n}' that are separated by an angle θ so that $\hat{n} \cdot \hat{n}' = \cos\theta$. By averaging over all such pairs, under the assumption that the fluctuations are Gaussian, we obtain the two-point correlation function, $C(\theta)$, which is written in terms of the multipole expansion

$$\langle \delta T(\hat{n}) \cdot \delta T(\hat{n}') \rangle \equiv C(\theta) = \sum_{\ell} \frac{(2\ell + 1)}{4\pi} C_{\ell} P_{\ell}(\cos\theta), \tag{45}$$

the C_{ℓ} coefficients are called the multipole moments.

As predicted, analysis of the temperature fluctuations does in fact reveal patterns corresponding to a harmonic series of longitudinal oscillations. The various modes correspond to the number of oscillations completed before recombination. The longest wavelength mode, subtending the largest angular size for the primary anisotropies, is the fundamental mode – this was the first mode detected. There is now strong evidence that both the 2nd and 3rd modes have also been observed [20-22].

The distance sound waves could have traveled in the time before recombination is called the *sound horizon*, r_s . The sound horizon is a fixed physical scale at the surface of last scattering. The size of the sound horizon depends on the values of the cosmological parameters.

The distance to the surface of last scattering, d_{sls} , also depends on cosmological parameters. Together, they determine the angular size of the sound horizon (see Fig. 3)

$$\theta_s \approx \frac{r_s}{d_{sls}}, \quad (46)$$

in the same way that the angle subtended by the planet Jupiter depends on both its size and distance from us. Analysis of the temperature anisotropies in the CMB determine θ_s and the cosmological parameters can be varied in r_s and d_{sls} to determine the best-fit results.

We can estimate the sound horizon by the distance that sound can travel from the big bang, $t = 0$, to recombination t_*

$$r_s(z_*; \Omega_b, \Omega_r) \approx \int_0^{t_*} c_s dt, \quad (47)$$

where z_* is the redshift parameter at recombination ($z_* \approx 1100$) [25], Ω_r is the density parameter for radiation (photons), c_s is the speed of sound in the photon-baryon fluid, given by [26]

$$c_s \approx c [3 (1 + 3\Omega_b/4\Omega_r)]^{-1/2}, \quad (48)$$

which depends on the baryon-to-photon density ratio, and dt is determined by an expression similar to Eq. (36), except at an epoch in which radiation plays a more important role. The energy density of radiation scales as $\rho_r \propto a^{-4}$ [27], so with the addition of radiation, Eq. (33) generalizes to

$$\left(\frac{da}{dt}\right)^2 = H_0^2 \left[\Omega_{r,0} \left(\frac{a_0}{a}\right)^2 + \Omega_{m,0} \frac{a_0}{a} + \Omega_{k,0} + \Omega_{\Lambda,0} \left(\frac{a}{a_0}\right)^2 \right], \quad (49)$$

which, upon using Eq. (35) and $\Omega_r + \Omega_m + \Omega_\Lambda + \Omega_k = 1$, leads to

$$dt = H_0^{-1} (1+z)^{-1} \left\{ (1+z)^2 (1 + \Omega_{m,0} z) + z(z+2) [(1+z)^2 \Omega_{r,0} - \Omega_{\Lambda,0}] \right\}^{-1/2} dz. \quad (50)$$

The distance to the surface of last scattering, corresponding to its angular size, is given by what is called the angular diameter distance. It has a simple relationship to the luminosity distance d [15] given in Eq. (37)

$$d_{sls} = \frac{d(z_*; \Omega_m, \Omega_\Lambda)}{(1 + z_*)^2}. \quad (51)$$

The location of the first acoustic peak is given by $\ell \approx d_{sls}/r_s$ and is most sensitive to the curvature of the universe Ω_k .

To get a feeling for this result, we can consider a very simplified, heuristic calculation. We will consider a prediction for the first acoustic peak for the case of a flat universe. To leading order, the speed of sound in the photon-baryon fluid, Eq. (48), is constant $c_s = c/\sqrt{3}$. We further make the simplifying assumption that the early universe was matter-dominated (there is good reason to believe that it was which will be discussed in the next section). With these assumptions, Eqs. (49) and (47) yield (dropping the ‘0’ from the density parameters)

$$r_s = \frac{c_s}{H_0 \sqrt{\Omega_m}} \int_{z_*}^{\infty} (1 + z)^{-5/2} dz, \quad (52)$$

which gives

$$r_s = \frac{2c_s}{3H_0 \sqrt{\Omega_m}} (1 + z_*)^{-3/2}. \quad (53)$$

The distance to the surface of last scattering, in our flat universe model, will depend on both Ω_m and Ω_Λ . Following a procedure similar to that which lead to Eq. (37), the radial coordinate of the surface of last scattering, r_{sls} (not to be confused with r_s), is determined by

$$r_{sls} = \frac{c}{H_0} \int_0^{z_*} [\Omega_m(1 + z)^3 + \Omega_\Lambda]^{-1/2} dz, \quad (54)$$

which does not yield a simple result. Using a binomial expansion, the integrand can be approximated as $\Omega_m^{-1/2}(1 + z)^{-3/2} - (\Omega_\Lambda/2\Omega_m^{3/2})(1 + z)^{-9/2}$ and the integral is more easily handled. The distance is then determined by $d_{sls} = r_{sls}/(1 + z_*)$ which gives

$$d_{sls} = \frac{2c}{7H_0(1 + z_*)} \left\{ 7\Omega_m^{-1/2} - 2\Omega_\Lambda\Omega_m^{-3/2} + O[(1 + z_*)^{-1/2}] \right\}. \quad (55)$$

Using $\Omega_\Lambda = 1 - \Omega_m$ and neglecting the higher order terms gives

$$d_{sls} \approx \frac{2c\Omega_m^{-1/2}}{7H_0(1 + z_*)} \left\{ 9 - 2\Omega_m^3 \right\}. \quad (56)$$

Combining Eqs. (53) and (56) to get our prediction for the first acoustic peak gives

$$\ell \approx \frac{d_{sls}}{r_s} \approx 0.74\sqrt{(1+z_*)} \{9 - 2\Omega_m^3\} \approx 221. \quad (57)$$

This result is consistent with the more detailed result that [28]

$$\ell \approx 200/\sqrt{1 - \Omega_k}, \quad (58)$$

where, in our calculation $\Omega_k = 0$. Equation (58) suggests that a measurement of $\ell \approx 200$ implies a flat universe. The BOOMERanG [22] collaboration found $\ell \approx 197 \pm 6$, and the MAXIMA-1 [21] collaboration measured $\ell \approx 220$. Additional simplified illustrations for how the cosmological parameters can be obtained from the acoustic peak can be found in Ref. 29.

Experimental results, such as those quoted above, are determined by plotting the power spectrum (power per logarithmic interval), $(\delta T_\ell)^2$, given by

$$(\delta T_\ell)^2 = \frac{\ell(\ell + 1)}{2\pi} C_\ell, \quad (59)$$

or by the square root of this quantity. The power spectrum may be quickly calculated for a given cosmological model using a code such as CMBFAST which is freely available online [30]. The solid curve in Fig. 4 was calculated using CMBFAST and the data points are only a representative few included to show the kind of agreement between theory and experiment that exists.

While the location of the first acoustic peak helps to fix Ω_k , other features of the power spectrum help to determine the baryon density. Since baryons are the primary cause of the gravitational potential wells that help generate the acoustic oscillations, they affect the power spectrum in several ways. The relative heights of the peaks are an indication of Ω_b in that an increase in baryon density results in an enhancement of the odd peaks. An increase in baryon density also leads to enhanced damping at higher multipoles [31].

It is important to recognize that the constraints on cosmological parameters obtained through this sort of analysis are correlated so that the range of possible values of Ω_Λ ,

for example, depends on what is assumed for the possible range of values of the Hubble constant. Therefore, it is customary to incorporate results from other observational (or theoretical) work in the analysis of the CMB data. With this in mind, we use the value of the Hubble constant stated in Eq. (30). Given this assumption, a combined study of the CMB anisotropy data from the BOOMERanG [22], MAXIMA-1 [21], and COBE-DMR [32] collaborations suggests the following values for the two cosmological parameters being considered here [33]:

$$\begin{aligned}\Omega_{k,0} &= 0.11 \pm 0.07 \\ \Omega_{b,0} &= 0.062 \pm 0.01.\end{aligned}\tag{60}$$

As with the type Ia supernova results, the best-fit CMB results predict an essentially flat universe. In fact, it is quite possible to adopt a model with $\Omega_k \equiv 0$ and still obtain a very good fit to the data along with reasonable values for the other cosmological parameters [33]. Again, the CMB data also provides values for additional cosmological parameters, but the curvature and baryon densities are perhaps the most accurately constrained at this time.

Even though the recent revolution in cosmology was ignited by the type Ia supernova and CMB anisotropy results, it is also important to acknowledge prior work toward constraining the cosmological parameters. This work includes investigations on gravitational lensing [34], large-scale structure [35], and the ages of stars, galaxies, and globular clusters [36]. Without this work, the ability to use the supernova and CMB data to place fairly tight restrictions on the major cosmological parameters would be significantly diminished.

VI. THE PICTURE OF OUR UNIVERSE

Given the results from observational cosmology discussed in the previous two sections we are now able to present a concrete picture of the universe, as opposed to the traditional array of models with very different properties. Taking a more comprehensive view, in Table 2 we present a set of cosmological parameters (without errors) that might be taken as the “best estimates” based on various observational and theoretical studies [37].

TABLE 2. Our best estimates of the cosmological parameters for the present-day universe and the primary sources we used to obtain them. If “theory” is listed as the source, we derived the value from other estimates by using the stated equation.

Parameter	Value	Primary Sources
Hubble Constant	$H_0 = 72 \text{ km}\cdot\text{s}^{-1}\cdot\text{Mpc}^{-1}$	[13]
Cosmological Constant	$\Omega_\Lambda = 0.70$	[16, 33]
Matter	$\Omega_m = 0.30$	[16, 33]
Baryonic matter	$\Omega_b = 0.04$	[33]
Dark matter	$\Omega_{CDM} = 0.26$	theory: Eq. (61)
Curvature	$\Omega_k = 0.00$	[16, 20-22, 33]
Deceleration parameter	$q_0 = -0.55$	theory: Eq. (39)

This set of parameters describes a flat universe the dynamics of which is dominated by two mysterious forms of energy, most prominently, the cosmological constant. So then, the long-standing debate over whether or not the cosmological term should be included in Einstein’s theory is over; not only should it be included, it dominates the universe. Although the debate over the existence of the cosmological constant has ended, the debate over its physical implications has just begun. Further comments about this debate will be discussed in the conclusion.

The other mysterious form of energy listed in Table 2, Ω_{CDM} , is dark matter where “CDM” stands for “cold dark matter.” Recall that ordinary matter made up of atomic nuclei only contributes to the baryon content of the universe with $\Omega_b \approx 0.04$. However, since the total matter content is $\Omega_m \approx 0.30$, the rest of the matter in the universe must be in some exotic, unseen form which is why we call it dark matter

$$\Omega_{CDM} = \Omega_m - \Omega_b \tag{61}$$

We have known about dark matter for several decades now, having been first discovered through anomalous rotation curves of galaxies [3]. The results from the CMB anisotropies only help to confirm that not only does dark matter exist, but that it comprises roughly 90% of the matter in the universe.

Given values of the cosmological parameters, we can now solve for the dynamics of the universe. The Friedmann equations (16) and (17) for our present ($p_m = 0$, $k = 0$) universe can be combined to give

$$2\frac{\ddot{a}}{a} + \left(\frac{\dot{a}}{a}\right)^2 = \Lambda c^2. \quad (62)$$

This equation can be solved exactly giving the result [38]

$$a(t) = A^{1/3} \sinh^{2/3}\left(\frac{t}{t_\Lambda}\right), \quad (63)$$

where $A = \Omega_{m,0}/\Omega_{\Lambda,0} \approx 0.43$ and $t_\Lambda = (4/3\Lambda c^2)^{1/2} \approx 3.4 \times 10^{17}$ s. The cosmic scale factor is plotted in Fig. 5 and compared to the purely de Sitter universe described by Eq. (20). From this comparison, we see that, today, the qualitative behavior of our universe is that of a de Sitter universe except that the presence of matter has caused the universe to expand less than in the de Sitter case.

With $a(t)$ in hand, we can now write a precise metric for the universe

$$ds^2 = c^2 dt^2 - A^{2/3} \sinh^{4/3}(t/t_\Lambda) \left[dr^2 + r^2 d\theta^2 + r^2 \sin^2 \theta d\phi^2 \right]. \quad (64)$$

This tells us that we can visualize the universe as an expanding Euclidean sphere with the expansion governed by $a(t)$ as given in Eq. (63). Note, however, that in this visualization the universe is represented as the entire volume of the sphere and not just the surface.

Another interesting feature that emerges from this picture is that if Λ is truly constant, the universe would have once been matter-dominated. To see why this is, recall that because the size of the universe changes, the density parameters are functions of time. As we go back in time, the universe gets smaller so that the energy density of matter ρ_m gets larger while the energy density associated with Λ , see Eq. (15), remains constant. Using Eq. (22) we can see that the ratio of matter-to-cosmological constant is

$$\frac{\Omega_m}{\Omega_\Lambda} = \frac{\Omega_{m,0}}{\Omega_{\Lambda,0}} a^{-3}(t). \quad (65)$$

Therefore, at some finite time in the past the universe was such that $\Omega_m/\Omega_\Lambda > 1$. Since the expansion of a matter-dominated universe would be decelerating, this implies that the universe underwent a transition from decelerated expansion to accelerated expansion. This behavior is reflected in the deceleration parameter as a function of time, which, given the current cosmological parameters becomes

$$q(t) = \frac{1}{2} \left[1 - 3 \tanh^2(t/t_\Lambda) \right]. \quad (66)$$

Figure 6 is a plot of $q(t)$ and shows that the deceleration parameter was once positive and that a transition to $q(t) < 0$ occurred around the time at which $\Omega_m/\Omega_\Lambda = 1$.

Having a specific model of the universe allows us to determine specific answers to questions that cosmologists have been asking for decades. While we cannot address all such questions in this paper we will tackle a few of the most common: (a) What is the age of the universe? (b) Will the universe expand forever or will the expansion eventually stop followed by a re-collapse? (c) Where is the edge of the observable universe?

The age of the universe can be calculated by integrating dt from now, $z = 0$, back to the beginning $z = \infty$. For our universe, the steps leading to Eq. (36) produces

$$dt = H_0^{-1} (1+z)^{-1} \left[\Omega_{m,0} (1+z)^3 + \Omega_{\Lambda,0} \right]^{-1/2} dz. \quad (67)$$

Making the definition $x \equiv 1+z$, the present age of the universe is given by

$$t_0 = H_0^{-1} \int_1^\infty \left[\Omega_{m,0} x^5 + \Omega_{\Lambda,0} x^2 \right]^{-1/2} dx. \quad (68)$$

The solution to Eq. (68) is complex. Taking only the real part gives

$$t_0 = \frac{2}{3H_0\Omega_{\Lambda,0}^{1/2}} \tanh^{-1} \left[\left(1 + \frac{\Omega_{m,0}}{\Omega_{\Lambda,0}} \right)^{1/2} \right] = 13.1 \times 10^9 \text{ yr}. \quad (69)$$

The question of whether or not the universe will expand forever is determined by the asymptotic behavior of $a(t)$. Since $\sinh(x)$ diverges as $x \rightarrow \infty$, it is clear that the universe will continue to expand indefinitely unless some presently unknown physical process drastically alters its dynamics.

Finally, concerning the question of the size of the observable universe, there are two types of horizons that might fit this description, the *particle horizon* and the *event horizon*. The particle horizon is the position of the most distant event that can presently be seen, that is, from which light has had enough time to reach us since the beginning of the universe. Unfortunately, since current evidence suggests that the universe was not always dominated by the cosmological constant, we cannot extend the current model back to the beginning. We can, however, extend it into the future. The event horizon is the position of the most distant event that we will ever see. If we consider a photon moving radially toward us from this event, then Eq. (31) describes its flight. Since we are interested in those events that will occur from now t_0 , onward, Eq. (31) leads to

$$\int_0^{r_{EH}} dr = cA^{-1/3} \int_{t_0}^{\infty} \sinh^{-2/3}(t/t_{\Lambda}) dt, \quad (70)$$

where r_{EH} is the radial coordinate of our event horizon. Performing a numerical solution to the integral yields

$$r_{EH} \approx 1.2ct_{\Lambda} = 16 \times 10^9 \text{ light years}. \quad (71)$$

This result suggests that 16 billion light years is the furthest that we will ever be able to see. As far as we are aware, the most distant object ever observed (besides the CMB) is currently the galaxy RD1 at a redshift of $z = 5.34$, which places it approximately 12.2 billion light years away [39].

VII. CONCLUSIONS

In summary, the recent observational results in cosmology strongly suggest that we live in a universe that is spatially flat, expanding at an accelerated rate, homogeneous and isotropic on large scales, and is approximately 13 billion years old. The expansion of the universe is described by Eq. (63), and its metric by Eq. (64). We have seen that roughly 96% of the matter and energy in the universe consists of cold dark matter and the cosmological

constant. We now know basic facts about the universe much more precisely than we ever have. However, since we cannot speak with confidence about the nature of dark matter or the cosmological constant, perhaps the most interesting thing about all of this is that knowing more about the universe has only shown us just how little we really understand.

As mentioned previously, the most common view of the cosmological constant is that it is a form of vacuum energy due, perhaps, to quantum fluctuations in spacetime [5]. However, within the context of general relativity alone there is no need for such an interpretation; Λ is just a natural part of the geometric theory [40]. If, however, we adopt the view that the cosmological constant belongs more with the energy-momentum tensor than with the curvature tensor, this opens up a host of possibilities including the possibility that Λ is a function of time [41].

In conclusion, it is also important to state that although this paper emphasizes what the recent results say about our present universe, these results also have strong implications for our understanding of the distant past and future of the universe. For an entertaining discussion of the future of the universe see Ref. 42. Concerning the past, the results on anisotropies in the CMB have provided strong evidence in favor of the inflationary scenario, which requires a Λ -like field in the early universe to drive the inflationary dynamics. To quote White and Cohn, “Of dozens of theories proposed before 1990, only inflation and cosmological defects survived after the COBE announcement, and only inflation is currently regarded as viable by the majority of cosmologists” [17].

VIII. ACKNOWLEDGEMENTS

We would like to acknowledge (and recommend) the excellent website of Dr. Wayne Hu [43]. This resource is very useful for learning about the physics of CMB anisotropies. We are also grateful to Dr. Manasse Mbonye for making several useful suggestions.

- [1] Steven Weinberg, *Gravitation and Cosmology: Principles and Applications of the General Theory of Relativity*, (John Wiley & Sons, New York, 1972).
- [2] It should be noted that what we have called the Hubble parameter is also often called the Hubble constant. This name is inappropriate, however, because the Hubble parameter is time dependent.
- [3] Vera Rubin, *Bright Galaxies, Dark Matter*, (Springer Verlag/AIP Press, New York, 1997).
- [4] P. J. E. Peebles, *Principles of Physical Cosmology*, (Princeton University Press, Princeton, 1993) p. 14.
- [5] Sean M. Carroll, “The Cosmological Constant,” *Living Rev. Rel.* **4**, 1-80 (2001); astro-ph/0004075.
- [6] For additional discussion on the cosmological constant see A. Harvey and E. Schucking, “Einstein’s mistake and the cosmological constant,” *Am. J. Phys.* **68**, 723-727 (2000).
- [7] Stephen Webb, *Measuring the Universe: The Cosmological Distance Ladder*, (Praxis, Chichester, UK, 1999), pp. 229-230.
- [8] P. Hofflich, Thielemann, F. K., and Wheeler J. C., “Type Ia Supernovae: Influence of the Initial Composition on the Nucleosynthesis, Light Curves, Spectra, and Consequences for the Determination of Ω_M & Λ ,” *Astrophys. J.* **495**, 617-629 (1998); astro-ph/9709233.
- [9] Bradley W. Carroll and Dale A. Ostlie, *An Introduction to Modern Astrophysics* (Addison-Wesley, Reading, MA, 1996) pp. 588-590.
- [10] M. Hamuy, M. M. Phillips, J. Maza *et al.*, “A Hubble Diagram of Distant Type Ia Supernovae,” *The Astron. Journal*, **109**(1), 1-13 (1995).
- [11] See p. 231 of Ref. 7.
- [12] M. Hamuy, M. M. Phillips, N. Suntzeff, and R. Schommer, “The Hubble Diagram of the Calán/Tololo Type Ia Supernovae and the value of H_0 ,” *The Astron. Journal*, **112**, 2398-2407

- (1996); astro-ph/9609062. A. G. Kim, S. Gabi, G. Goldharber *et al.* “Implications for the Hubble Constant from the First Seven Supernovae at $z \leq 0.35$,” *Astrophys. J.* **476**, L63-66 (1997).
- [13] Wendy L. Freedman, B. F. Madore, B. K. Gibson *et al.*, “Final Results from the Hubble Space Telescope Key Project to Measure the Hubble Constant,” *Astrophys. J.*, **553**, 47-72 (2001).
- [14] See p. 97 of Ref. 4.
- [15] S. M. Carroll, W. H. Press, and E. L. Turner, “The Cosmological Constant,” *Ann. Rev. Astron. & Astrophys.*, **30**, 499-542 (1992).
- [16] Adam G. Riess, Alexei V. Filippenko, Peter Challis *et al.*, “Observational Evidence from Supernovae for an Accelerating Universe and a Cosmological Constant,” *Astron. J.*, **116**, 1009-1038 (1998).
- [17] Martin White and J. D. Cohn, “Resource Letter: TACMB-1: The theory of anisotropies in the cosmic microwave background,” *Am. J. Phys.* **70**, 106-118 (2002).
- [18] Alan H. Guth, *The Inflationary Universe*, (Perseus Books, Reading, MA, 1997).
- [19] G. F. Smoot, C. L. Bennett, A. Kogut *et al.*, “Structure in the COBE differential microwave radiometer first-year maps,” *Astrophys. J.* **396**, L1-5 (1992).
- [20] A. D. Miller, R. Caldwell, M. J. Devlin *et al.*, “A Measurement of the Angular Power Spectrum of the Cosmic Microwave Background from $l = 100$ to 400,” *Astrophys. J.*, **524**, L1-4 (1999); astro-ph/9906421.
- [21] S. Hanany, P. Ade, A. Balbi *et al.*, “MAXIMA-1: A Measurement of the Cosmic Microwave Background Anisotropy on Angular Scales of $10' - 5^\circ$,” *Astrophys. J.*, **545**, L5-9 (2000); astro-ph/0005123.
- [22] P. de Bernardis, P. A. R. Ade, J. J. Bock *et al.*, “A Flat Universe from High-resolution Maps of the Cosmic Microwave Background Radiation,” *Nature*, **404**, 955-959 (2000); astro-ph/0004404.
- [23] J. A. Peacock, *Cosmological Physics*, (Cambridge University Press, New York, 1999) pp. 591-592.

- [24] P. J. E. Peebles and J. T. Yu, “Primeval Adiabatic Perturbation in an Expanding Universe,” *Astrophys. J.*, **162**, 815-836 (1970).
- [25] Martin White, Douglas Scott, and Joseph Silk, “Anisotropies in the Cosmic Microwave Background,” *Ann. Rev. Astron. Astrophys.*, **32**, 319-370 (1994).
- [26] W. Hu and M. White, “Acoustic Signatures in the Cosmic Microwave Background,” *Astrophys. J.*, **471**, 30-51 (1996); astro-ph/9602019.
- [27] Hans C. Ohanian and Remo Ruffini, *Gravitation and Spacetime*, 2nd ed., (W. W. Norton & Co., New York, 1994) chap. 10.
- [28] See Ref. 21.
- [29] Neil J. Cornish, “Using the acoustic peak to measure cosmological parameters,” *Phys. Rev. D*, **63**, 027302-1 - 4 (2001); astro-ph/0005261.
- [30] See <http://physics.nyu.edu/matiasz/CMBFAST/cmbfast.html>
- [31] See Ref. 26.
- [32] C. L. Bennett, A. J. Banday, K. M. Górski *et al.*, “Four-Year COBE DMR Cosmic Microwave Background Observations: Maps and Basic Results,” *Astrophys. J.*, **464**, L1-4 (1996).
- [33] A. H. Jaffe, P. A. R. Ade, A. Balbi *et al.*, “Cosmology from MAXIMA-1, BOOMERANG & CODE/DMR CMB Observations,” *Phys. Rev. Lett.*, **86**, 3475-3479 (2001); astro-ph/0007333.
- [34] Kyu-Hyun Chae, “New Modeling of the Lensing Galaxy and Cluster of Q0957+561: Implications for the Global Value of the Hubble Constant,” *Astrophys. J.*, **524**, 582-590 (1999).
- [35] J. A. Peacock, S. Cole, P. Norberg *et al.*, “A measurement of the cosmological mass density from clustering in the 2dF Galaxy Redshift Survey,” *Nature*, **410**, 169-173 (2001); astro-ph/0103143.
- [36] L. M. Krauss, “The Age of Globular Clusters,” *Phys. Rept.*, **333**, 33-45 (2000); astro-ph/9907308.

- [37] The values that we have used are predominantly consistent with those of C. H. Linewater, “Cosmological Parameters,” astro-ph/0112381.
- [38] Ø. Grøn, “A new standard model of the universe,” *Eur. J. Phys.* **23**, 135-144 (2002).
- [39] A. Dey, H. Spinrad, D. Stern *et al.*, “A galaxy at $z = 5.34$,” *Astrophys. J.*, **498**, L93-97 (1998).
- [40] See, for example, Alex Harvey, “Is the Universe’s Expansion Accelerating?,” *Phys. Today (Letters)*, **55**, 73-74 (2002).
- [41] See for example, M. Doran and C. Wetterich, “Quintessence and the cosmological constant,” astro-ph/0205267; and M. Mbonye, “Matter fields from a decaying background Lambda vacuum,” astro-ph/0208244.
- [42] Fred Adams and Greg Laughlin, *The Five Ages of the Universe: Inside the Physics of Eternity*, (Simon & Schuster, New York, 1999).
- [43] See <http://background.uchicago.edu/~whu/>.

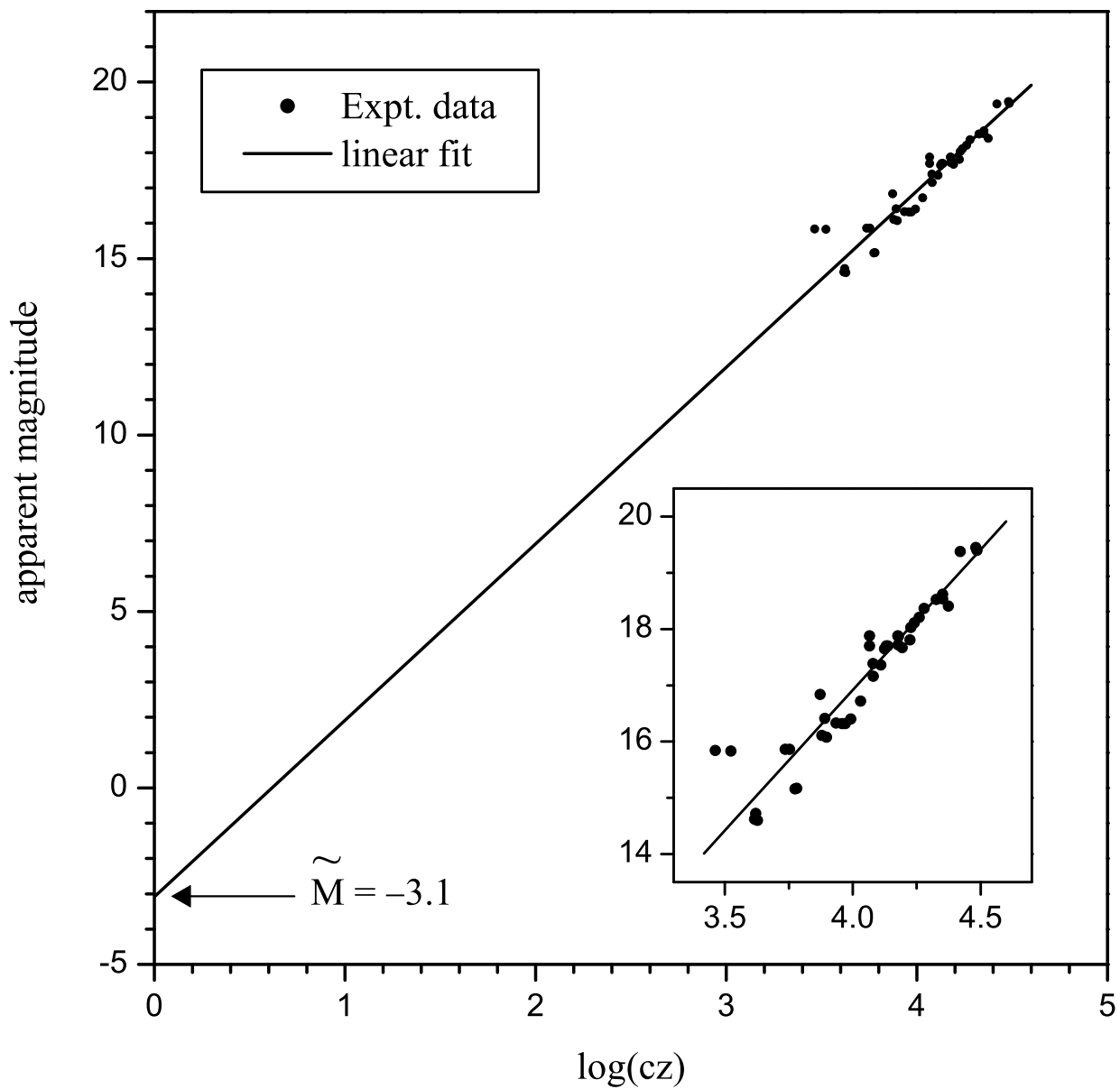


FIGURE 1. Using low-redshift supernovae to determine the Hubble constant. The data points are from Ref. 12. The inset graph shows a close-up view of the data and the best-fit line. The best-fit line determines the intercept which can be used in Eq. (28) to determine the Hubble constant.

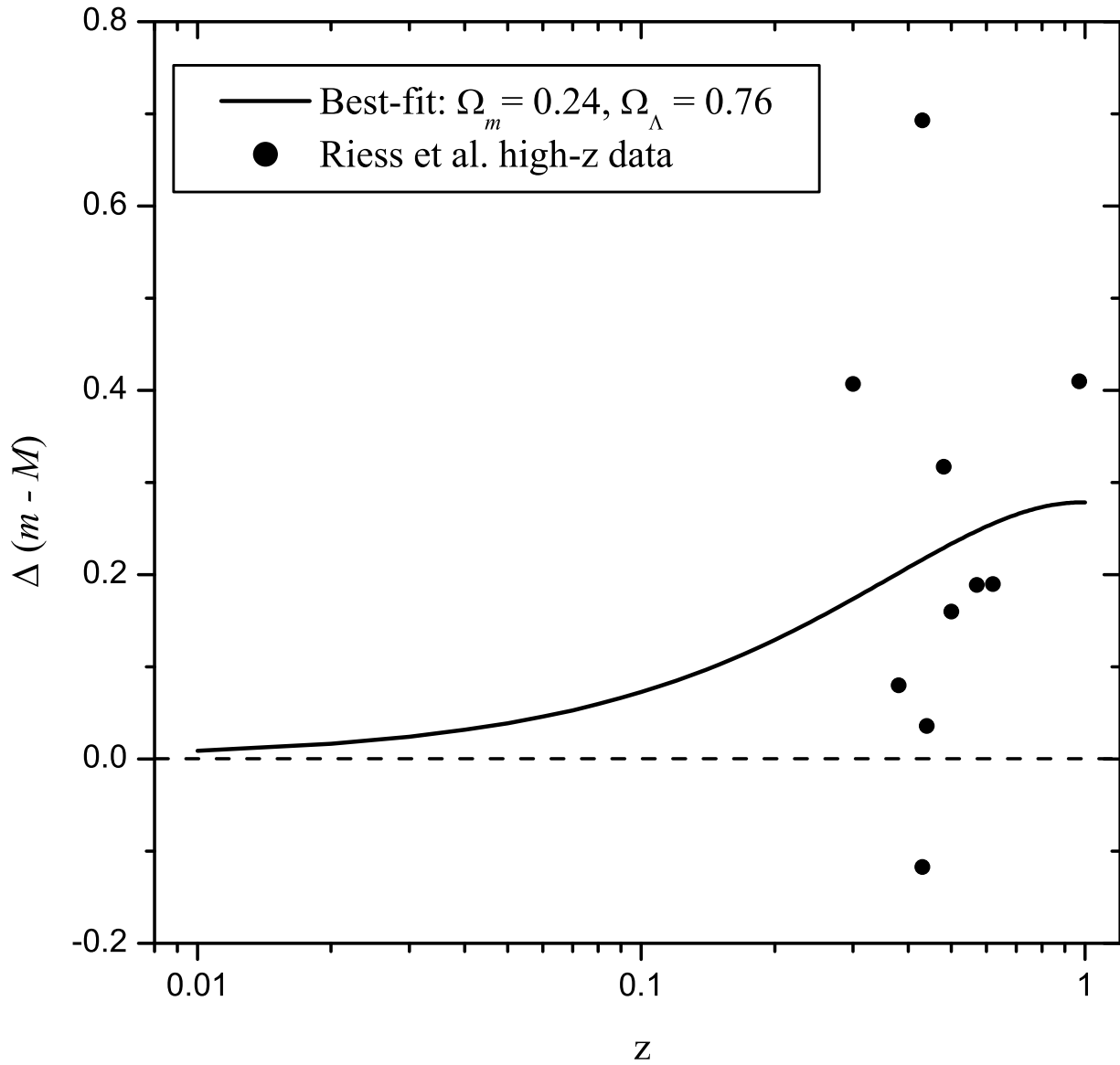


FIGURE 2. Using high-redshift data to determine cosmological parameters and provide evidence for a nonzero cosmological constant. The zero line corresponds to a traditional decelerating model of the universe with $\Omega_m = 0.2$, $\Omega_\Lambda = 0$, and $\Omega_k = 0.8$. The data points are the high-redshift supernovae from Ref. 16. The solid curve corresponds to those cosmological parameters that produce a best fit to the data points as determined in Ref. 16.

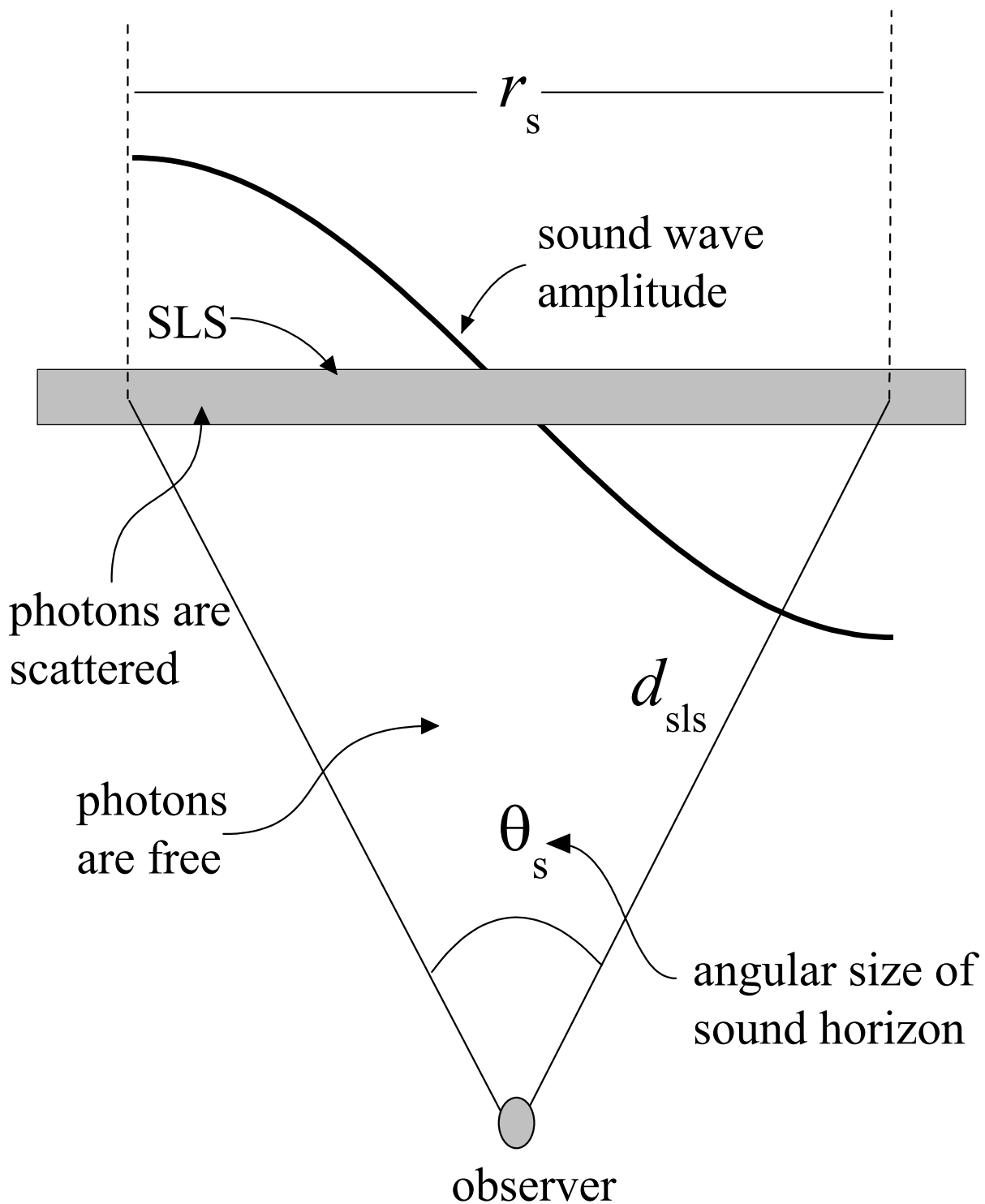


FIGURE 3. The surface of last scattering (SLS), the fundamental acoustic mode, and the sound horizon (r_s , θ_s). The photons of the CMB underwent Thomson scattering in the early universe and acoustic oscillation left their imprint at recombination.

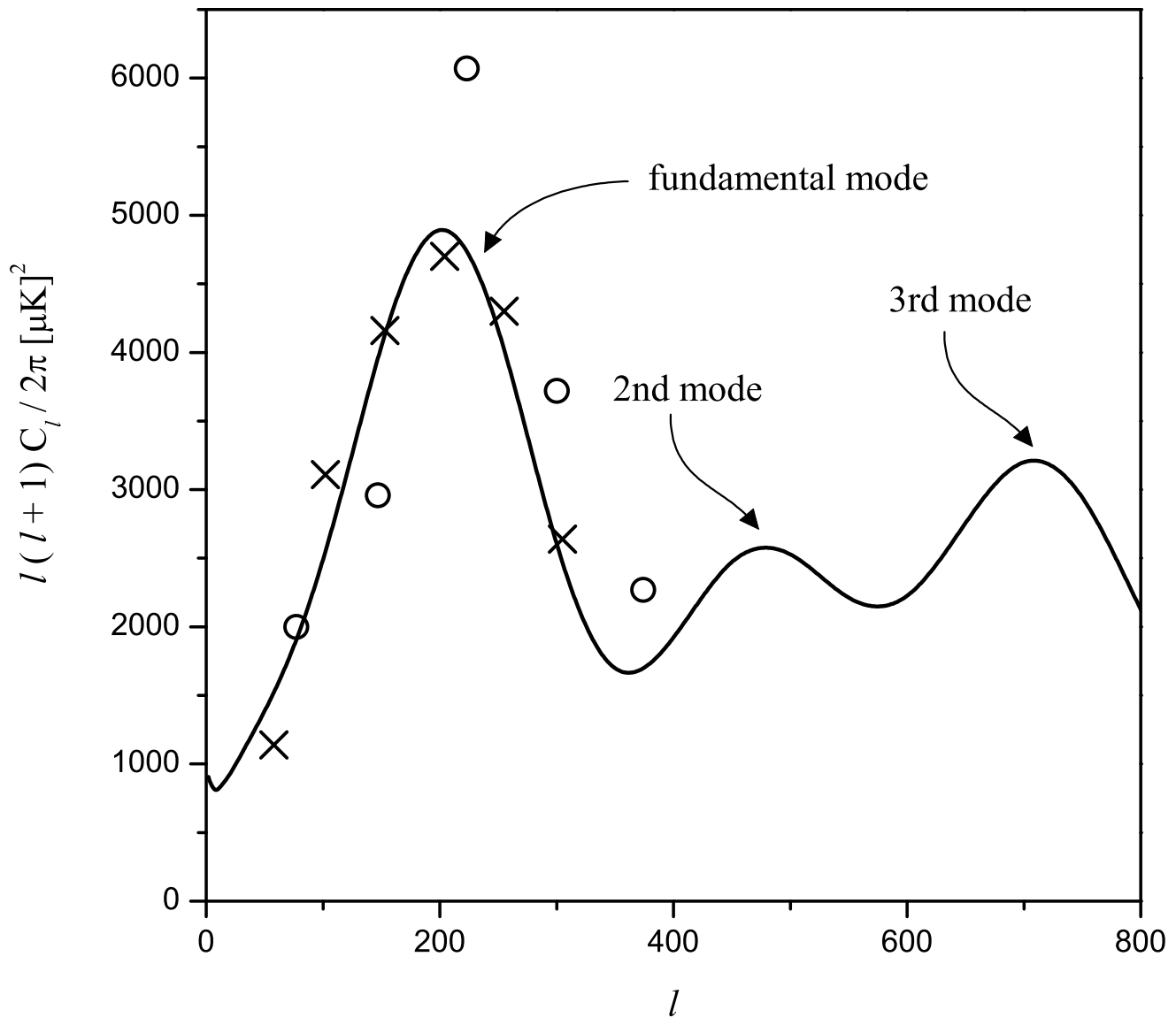


FIGURE 4. The power spectrum. The solid curve is a theoretical power spectrum calculated using CMBFAST [30]. The open circles are from Ref. 20 and the crosses are from Ref. 21. Notice that the first peak corresponding to the fundamental acoustic mode occurs near $l = 200$, signifying a flat universe.

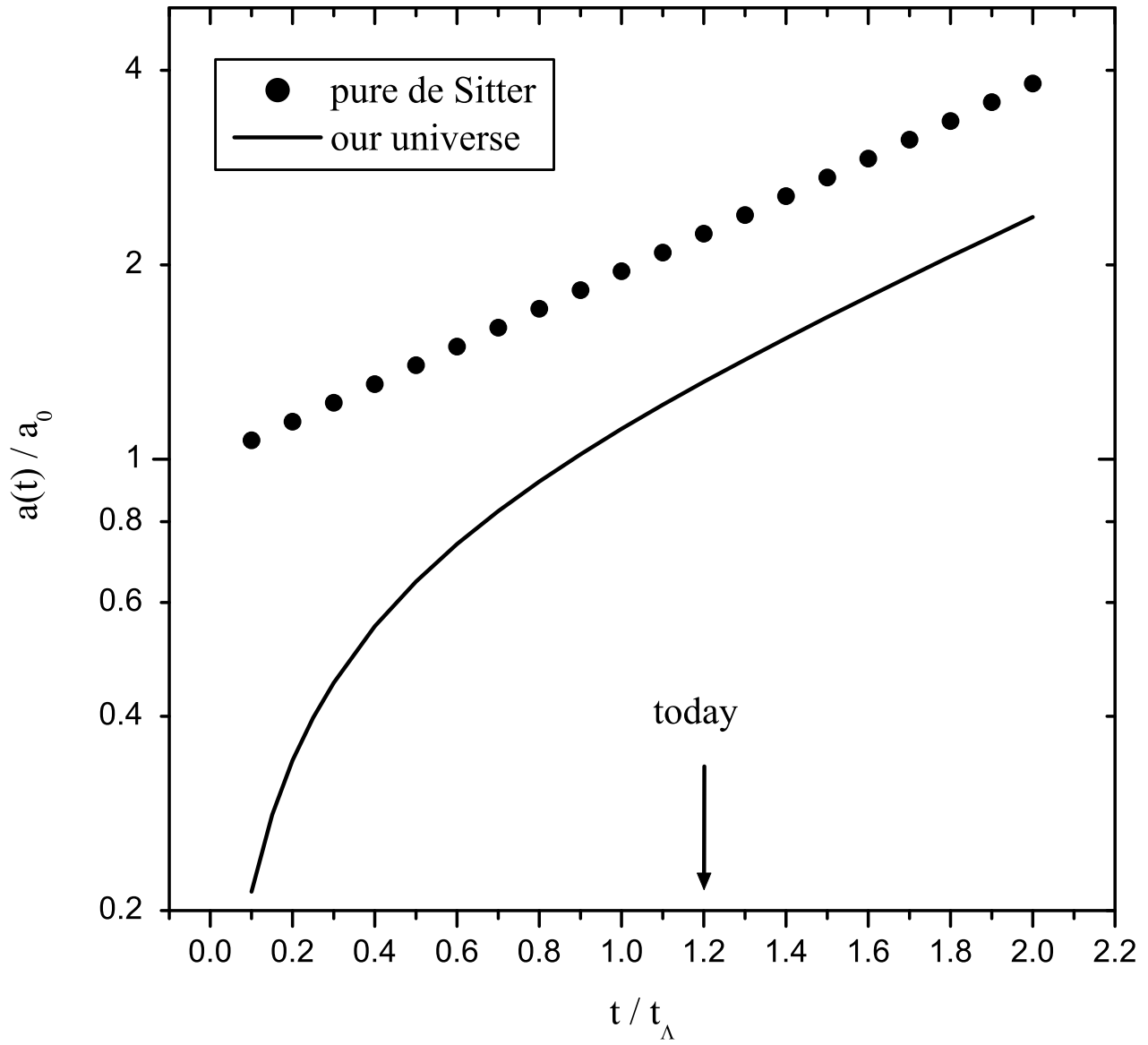


FIGURE 5. The cosmic scale factor for our universe compare to the de Sitter model.

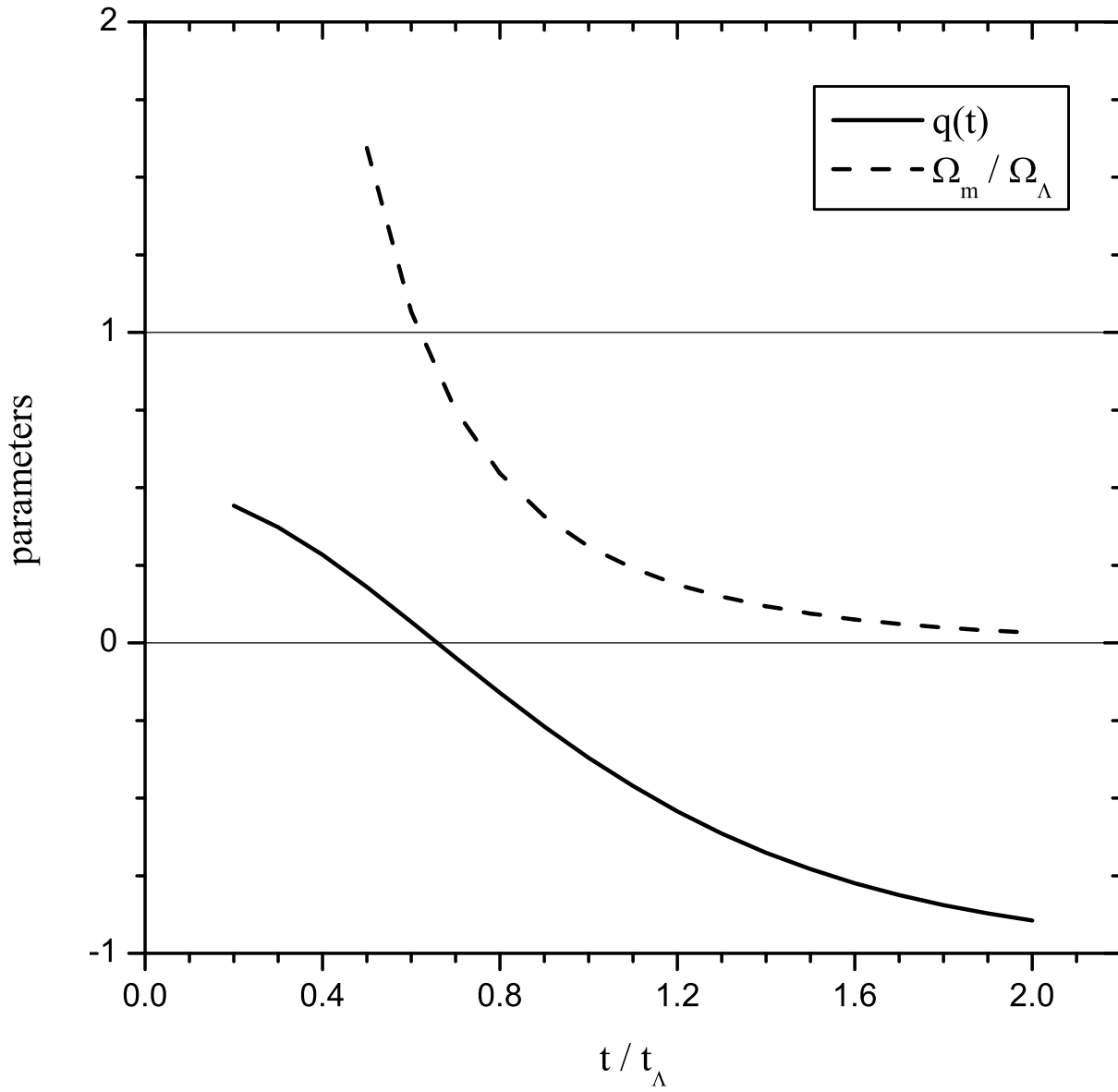


FIGURE 6. The deceleration parameter of our universe. The sign of $q(t)$ switches from positive to negative at around the same time that the universe goes from matter-dominated to Λ -dominated.